Array 17 (2023) 100265

Contents lists available at ScienceDirect

Array

journal homepage: www.elsevier.com/locate/array

Nonlinear anisotropic diffusion methods for image denoising problems: Challenges and future research opportunities

Baraka Maiseli

Department of Electronics & Telecommunications Engineering, College of Information & Communication Technologies, University of Dar es Salaam, P.O. Box 33335, Dar es Salaam, Tanzania

ARTICLE INFO

Dataset link: https://www.mathworks.com/matlabcentral/fileexchange/116260-anisotropic-diffusion-denoising

Keywords:
Anisotropic diffusion
Image processing
Inverse problem
Noise estimation
Restoration method

ABSTRACT

Nonlinear anisotropic diffusion has attracted a great deal of attention for its ability to simultaneously remove noise and preserve semantic image features. This ability favors several image processing and computer vision applications, including noise removal in medical and scientific images that contain critical features (textures, edges, and contours). Despite their promising performance, methods based on nonlinear anisotropic diffusion suffer from practical limitations that have been lightly discussed in the literature. Our work surfaces these limitations as an attempt to create future research opportunities. In addition, we have proposed a diffusion-driven method that generates superior results compared with classical methods, including the popular Perona–Malik formulation. The proposed method embeds a kernel that properly guides the diffusion process across image regions. Experimental results show that our kernel encourages effective noise removal and ensures preservation of significant image features. We have provided potential research problems to further expand the current results.

1. Introduction

Noise, regardless of its source and type, degrades the quality of images, making them less useful in sensitive applications [1–3]. For example, noise may corrupt the details of a medical image and cause doctors to incorrectly interpret results of patients. In computer and machine vision applications, noisy images may negatively impact the accuracy and reliability of the object detection and recognition algorithms. Motivated by the quest for quality images in a wide range of applications, there has been intensive efforts to develop different methods for suppressing noise in images [4–13].

Noise may be generated during acquisition, processing, and transmission of an image. For instance, if the imaging sensor contains damaged pixels on its surface, random spots (noises) with varied intensities will be introduced into the acquired image because such locations cannot register the incident light. Examples of noise in images include salt & pepper [14], Gaussian [15,16], Poisson [17], shot [18], and speckle [2,19], typically modeled as either additive (noise added to the original image) or multiplicative (noise multiplied to the original image).

Several image denoising methods adapted for a range of noise types have been proposed in the literature [20–23]. Of the methods, those based on anisotropic diffusion processes have gained a considerable attention for the ability of such methods to simultaneously remove noise and preserve semantically useful image features (textures, edges, and contours) [24–27]. The seminal work by Perona and Malik [28] has inspired many scholars to develop advanced anisotropic diffusion models for suppressing spurious image features, including noise and undesirable artifacts. These models have demonstrated outstanding results in delicate image denoising applications (e.g., medical imaging) that require quality images with critical features well preserved.

Despite the merits of anisotropic diffusion processes in image denoising, scholars have not adequately unraveled the possible research opportunities to advance the field. This work opens scholarly discussions to address various limitations of the available anisotropic diffusion models. We highlight recommendations for the possible solutions of some limitations as guidance for scholars. Furthermore, a superior method based on nonlinear anisotropic diffusion process is proposed. Compared with classical methods, our method demonstrates outstanding results by generating images with higher perceptual and objective qualities. Some recommendations are provided to further expand the our results.

We have organized our paper as follows: the next section extensively reviews anisotropic diffusion when applied in image denoising; Section 3 gives potential research avenues in anisotropic diffusion, providing researchers with immense opportunities to advance this growing field; Section 4 describes our anisotropic diffusion method

E-mail address: barakaezra@udsm.ac.tz.

https://doi.org/10.1016/j.array.2022.100265
Received 20 September 2022; Received in revised form 16 November 2022; Accepted 17 November 2022
Available online 21 November 2022

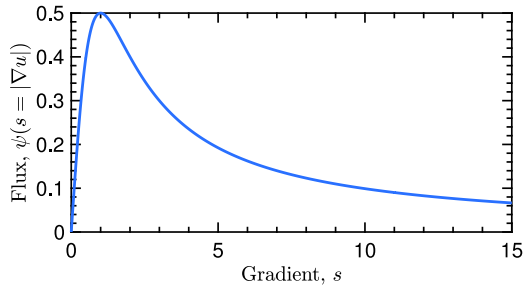

Fig. 1. Perona–Malik influence functional (flux) versus image gradient: $\psi(s) = \frac{s}{1+\left(\frac{s}{K}\right)^2}$, $K = 1$.

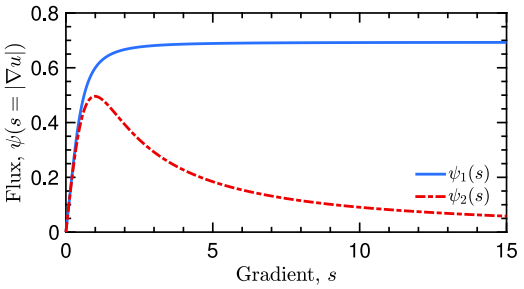

Fig. 2. Our influence functionals versus image gradient: $\psi_1(s) = s\left(\frac{1-a^{-\left(\frac{1}{K}\right)}}{1+a^{-\left(\frac{1}{K}\right)}}\right)$ and $\psi_2(s) = s\left(\frac{a^{-\left(\frac{s}{K}\right)}}{1+\left(\frac{s}{K}\right)^2}\right)$.

and highlights its competitive advantages; Section 5 presents and discusses results; finally, we have concluded the research in Section 6 by summarizing our study and proving perspectives.

2. Anisotropic diffusion in image processing

In science and engineering disciplines, diffusion generally means movement of particles (e.g., atoms, ions, and molecules) between regions of different concentrations until equilibrium conditions are established. This physical process may be explained by the *Fick's law*

$$j = -D \cdot \nabla u, \tag{2.1}$$

which states that the concentration gradient, ∇u, generates flux, j, with a goal of compensating for this gradient at the rate governed by the diffusion tensor (positive definite symmetric matrix), D [29] (Figs. 1 and 2). The process dictates particles from the highly concentrated region to move at the rate determined by D towards the region of low concentration. Diffusion obeys the fundamental laws of mass conservation, hence the process does not lead to creation or destruction of mass, u, as described by the *continuity equation*

$$\frac{\partial u}{\partial t} = -\mathrm{div} j, \tag{2.2}$$

with t denoting time. Plugging (2.2) into (2.1) gives the diffusion equation

$$\frac{\partial u}{\partial t} = \mathrm{div}(D \cdot \nabla u) \tag{2.3}$$

that models several physical processes involving mass transportation (e.g., carburization and construction of semiconductors through doping).

In image processing and computer vision, u denotes the intensity of an image. Therefore, applying (2.1) on the image dictates movement of intensity from high-intensity to low-intensity pixels. This process causes smoothing where the intensity of image regions with spurious features (noise) gets reduced.

The directions of j and ∇u determine the type of diffusion: parallel, isotropic; and non-parallel, anisotropic. The formulation (2.1) resembles the heat flow equation (or convolution of u with a Gaussian kernel) when D remains constant over all image regions that undergo isotropic diffusion. Setting D constant tends to smudge edges and other critical image features, a consequence not preferred in many sensitive applications. In anisotropic diffusion, D becomes a function of u, allowing it to change spatially across different image regions. For example, $D = f(|\nabla u|)$ may be a function of the image gradient to give the anisotropic diffusion equation

$$\frac{\partial u}{\partial t} = \mathrm{div}(f(|\nabla u|)\nabla u). \tag{2.4}$$

A well-designed f leads to image denoising with edge preservation.

Modeling noise as energy, ρ, in the image, we may regard diffusion as the energy minimization problem with a solution that represents a clean image of the lowest possible (global minimum) energy. Subsequently, (2.4) can be derived from the variational minimization problem

$$\arg\min_{u\in\Omega}\left\{\int_\Omega \rho(|\nabla u|)d\Omega\right\}, \tag{2.5}$$

where Ω denotes the domain of u. For completeness, and without loss of generality, (2.5) usually incorporates a fidelity energy functional (regularization term), ϑ, as

$$\arg\min_{u\in\Omega}\left\{\int_\Omega \rho(|\nabla u|)dx + \lambda\int_\Omega \vartheta(u,f)dx\right\}, \tag{2.6}$$

where λ represents a fidelity parameter that controls a trade-off between regularization (noise removal) and data fidelity. Large value of λ encourages smoother solutions, in which case regularization dominates over total energy. Furthermore, with a small value of λ, u approaches the observed noisy image, f.

The Euler–Lagrange equation corresponding to the energy functional (2.6) is

$$0 = -\mathrm{div}\left(\frac{\rho'(|\nabla u|)}{|\nabla u|}\nabla u\right) + \lambda\vartheta'(u,f), \quad x\in\Omega, \tag{2.7}$$

$$\frac{\partial u}{\partial \vec{n}} = 0, \quad x\in\partial\Omega. \tag{2.8}$$

Embedding (2.7) into a dynamical scheme gives

$$\frac{\partial u}{\partial t} = \mathrm{div}\left(\frac{\rho'(|\nabla u|)}{|\nabla u|}\nabla u\right) - \lambda\vartheta'(u,f), \quad (x,t)\in\Omega\times(0,T), \tag{2.9}$$

$$u(x,0) = f(x), \quad x\in\Omega \tag{2.10}$$

$$\frac{\partial u}{\partial \vec{n}} = 0, \quad (x,t)\in\partial\Omega\times[0,T]. \tag{2.11}$$

The parameter T denotes the maximum evolution time. Considering the divergence term of (2.9), $f(|\nabla u|) = \frac{\rho'(|\nabla u|)}{|\nabla u|}$ means diffusivity (diffusion coefficient) that governs the rate of noise removal as the solution, u, evolves.

We have selected [39]

$$\vartheta(u,f) = \log u + \frac{f}{u} \tag{2.12}$$

for its superior performance in dealing with both additive and multiplicative types of noise. Nevertheless, this energy functional of the fidelity term performs even better in images corrupted by multiplicative noise. Plugging $\vartheta(u,f)$ into (2.9) yields

$$\frac{\partial u}{\partial t} = \mathrm{div}\left(\frac{\rho'(|\nabla u|)}{|\nabla u|}\nabla u\right) - \lambda\frac{u-f}{u^2}, \quad (x,t)\in\Omega\times(0,T), \tag{2.13}$$

$$u(x,0) = f(x), \quad x\in\Omega \tag{2.14}$$

$$\frac{\partial u}{\partial \vec{n}} = 0, \quad (x,t)\in\partial\Omega\times[0,T]. \tag{2.15}$$

Most advances in anisotropic diffusion methods revolve around two directions: (1) design of ρ; and (2) estimation of ϑ according to the noise

Table 1
Energy functionals for anisotropic diffusion equations: $\rho(s = |\nabla u|)$, energy functional; $\psi(s) = \rho'(s)$, influence function; $\phi(s)$, diffusivity.

Nomenclature	$\rho(s)$	$\psi(s)$	$\phi(s)$	Comments
ℓ_2 [30]	$\frac{1}{2}s^2$	s	1	
ℓ_1 [31]	s	$\text{sgn}(s)$	$\frac{1}{s}$	
$\ell_1 - \ell_2$ [32]	$K^2\left(\sqrt{1+\left(\frac{s}{K}\right)^2}-1\right)$	$\frac{s}{\sqrt{1+\left(\frac{s}{K}\right)^2}}$	$\frac{1}{\sqrt{1+\left(\frac{s}{K}\right)^2}}$	$K \in \mathbb{R}^+$
ℓ_p [33]	$\frac{s^\nu}{\nu}$	$\text{sgn}(s)s^{\nu-1}$	$s^{\nu-2}$	$0 < \nu \leq 2$
"Fair"	$K^2\left[\frac{s}{K} - \log\left(1+\frac{s}{K}\right)\right]$	$\frac{s}{1+\frac{s}{K}}$	$\frac{1}{1+\frac{s}{K}}$	
Huber [34]	$\begin{cases}\frac{1}{2}s^2 \\ K\left(s-\frac{1}{2}K\right)\end{cases}$	$\begin{cases}s \\ K\text{sgn}(s)\end{cases}$	$\begin{cases}1 \\ \frac{K}{s}\end{cases}$	$\begin{cases}\text{if} \quad s \leq K \\ \text{if} \quad s > K\end{cases}$
Cauchy [28]	$\frac{K^2}{2}\log\left(1+\left(\frac{s}{K}\right)^2\right)$	$\frac{s}{1+\left(\frac{s}{K}\right)^2}$	$\frac{1}{1+\left(\frac{s}{K}\right)^2}$	
Geman–McClure [35,36]	$\frac{s^2}{2(1+s^2)}$	$\frac{s}{(1+s^2)^2}$	$\frac{1}{(1+s^2)^2}$	
Welsch [37]	$\frac{K^2}{2}\left[1-\exp\left(-\left(\frac{s}{K}\right)^2\right)\right]$	$s\exp\left(-\left(\frac{s}{K}\right)^2\right)$	$\exp\left(-\left(\frac{s}{K}\right)^2\right)$	
Tukey [38]	$\begin{cases}\frac{K^2}{6}\left(1-\left[1-\left(\frac{s}{K}\right)^2\right]^3\right) \\ \frac{K^2}{6}\end{cases}$	$\begin{cases}s\left[1-\left(\frac{s}{K}\right)^2\right]^2 \\ 0\end{cases}$	$\begin{cases}\left[1-\left(\frac{s}{K}\right)^2\right]^2 \\ 0\end{cases}$	$\begin{cases}\text{if} \quad s < K \\ \text{if} \quad s \geq K\end{cases}$
weighted $\ell_1 - \ell_2$	$CK^2\left(\sqrt{\left(1+\left(\frac{s}{K}\right)^2\right)}-1\right)$	$\frac{Cs}{\sqrt{1+\left(\frac{s}{K}\right)^2}}$	$\frac{C}{\sqrt{1+\left(\frac{s}{K}\right)^2}}$	$0 < C \leq 3.5$

statistics. In the former direction, scholars strive to design effective energy functionals with better mathematical properties, including convexity and uniqueness. Quality of the optimal solution of (2.9) depends on the design of ρ. The later direction requires a solid understanding of the noise statistics in the image. Performance of the anisotropic diffusion model depends upon how well ϑ adapts to the noise type (e.g., additive, multiplicative, and mixed).

3. Potential research avenues in anisotropic diffusion

3.1. Design of energy functionals

Formulation of an effective anisotropic diffusion equation requires a solid understanding of its corresponding energy functional, ρ. Superior denoising results may be achieved when ρ possesses proper mathematical properties, such as convexity and uniqueness. specifically, the variational problem governing ρ should guarantee existence and uniqueness of the minimizer, $u \in \Omega$, in (2.6). Despite these important requirements, no systematic procedures have been established to design ρ. Scholars have proposed different energy functionals (Table 1) without clear guidelines on what it takes to derive such functionals. Some interesting questions for further investigation would be (1) does an optimal ρ exist for all denoising applications? (2) what are systematic procedures for designing ρ? (3) what specific mathematical properties should be considered when designing ρ for denoising problems? (4) how does ρ behave at different scale resolutions of the evolving solution, u?

We noted a general practice that most authors design diffusivity functionals, $\phi(s) = \rho'(s)/s$, directly without considering the properties of ρ. This approach seems straightforward because $\phi(s)$ possesses a well-known mathematical property [28]: non-negative monotonically decreasing functional with $\phi(0) = 1$ and $\phi(\infty) = 0$. Perona and Malik [28] highlight that any well-designed $\phi(s)$ with this property may generate satisfactory results. However, it may not always be possible to derive ρ from $\phi(s)$ to learn the properties of ρ—an important functional to explain why the anisotropic diffusion equation works. For example, Guo et al. [40] proposed

$$\phi(s) = \frac{1}{1+\left(\frac{s}{K}\right)^\alpha}, \tag{3.1}$$

where K denotes the shape-defining tuning constant and $\alpha \in [0, 1]$ defines an adaptive variable exponent that changes according to the local image features. Although $\phi(s)$ proposed by Guo et al. generates convincing practical results, the corresponding formulation for

$$\rho(s) = \int_\Omega s\phi(s)dx \tag{3.2}$$

cannot produce a closed-form solution to associate ρ and quality of the results. Guo et al. explain that their anisotropic diffusion model outperforms because α changes adaptively to produce different other models during the diffusion process: linear, $\alpha = 0$; Total Variation, $\alpha = 1$; and Perona–Malik, $\alpha = 2$. This explanation, however, lacks scientific justification and generalization that changing α adaptively always lead to better results. We cannot state mathematically how the model behaves when α becomes a fraction, linking quality of results and the diffusion process. In addition, the authors did not provide the relationship between α and local image features: which value of α—translating to the anisotropic diffusion model (linear, Total Variation, or Perona–Malik)—should be applied to an image region for optimal denoising results?

In this work, we propose two diffusivity functionals, namely

$$\phi_1(s) = \frac{1-a^{-\frac{1}{\left(\frac{s}{K}\right)}}}{1+a^{-\frac{1}{\left(\frac{s}{K}\right)}}} \tag{3.3}$$

and

$$\phi_2(s) = \frac{a^{-\left(\frac{s}{K}\right)}}{1+\left(\frac{s}{K}\right)^2}, \tag{3.4}$$

where $a > 0$ denotes a constant, which generate promising results. These functionals, derived empirically through experiments, satisfy the conditions highlighted by Perona and Malik [28]:

$$\phi_1(s) = \phi_2(s) = \begin{cases}0 & \text{if} \quad s \to \infty \quad \text{(Edges and contours)} \\ 1 & \text{if} \quad s \to 0 \quad \text{(Flat regions)}\end{cases} \tag{3.5}$$

Eq. (3.4), with $a = 2.7183$ (exponential function), reduces to the functional similar to that proposed by Perona and Malik [28].

There could be several other variations of diffusivity functionals with outstanding performance. However, studies are yet to provide systematic mathematical procedures to establish such functionals. Therefore, although ϕ_1 and ϕ_2 proposed in this work performs well, we cannot mathematically confirm that they produce optimal results with respect to all variants of diffusivity functionals. This research direction may be interesting and worth investigating to advance denoising methods based on anisotropic diffusion.

3.2. Design of shape-defining constant

The diffusivity Eq. (3.1) contains a shape-defining constant, K, the threshold parameter of the gradient magnitude. This tuning constant controls the sensitivity of diffusion to edges, and is usually determined experimentally or as a function of the noise statistics in the image [41–44]. Quality of the denoised image depends, to a greater extent, on the value of K. Therefore, effective strategies are needed to optimize K for better denoising results. However, the available approaches for determining K are manual, hence time-consuming, inconvenient, and error-prone. Scholars may need to investigate the relationship between K and the structural information in the images. One interesting finding could be the value of K that changes adaptively depending upon the local image features, and this value should work across all types of images.

3.3. Design of regularization term

There have been efforts to design regularization (fidelity) terms for different noise types (e.g., additive and multiplicative) [45–50]. Due to the random nature of noise, designing regularization terms remains an open-ended research question and a non-trivial task. Given a noisy image, an interesting question would be to estimate the probability density function (PDF) that generates noise contained in the image. Noise models assume specific PDFs [51–53]: Gaussian, Gamma, Rayleigh, exponential, impulse, uniform, among others. Establishment of the regularization term requires a comprehensive understanding and analysis of these PDFs. In some situations, experiments should be performed to establish the relationship between noise statistics and structural information in the image.

Another aspect worth considering is the fidelity parameter, λ, of the regularization term, which is usually determined empirically. The manual strategy of tuning λ introduces challenges in the implementation of anisotropic diffusion models. Some authors have, however, recommended adaptive approaches for determining λ as the denoising image, u, evolves through iterations [40,54]. Guo et al. [40], for example, estimates λ by evaluating its value from (2.9) under steady conditions (when time tends to infinity). This approach implies that a more accurate value of λ may be obtained after convergence of the solution. Advanced techniques are needed to accurately determine λ after every iteration. We may investigate structural features and noise statistics of previous (premature) solutions to estimate λ iteratively.

3.4. Applications in inverse problems

Given observations from the system under investigation, an inverse problem involves determination of parameters characterizing the system [55–57]. For example, the image denoising problem provides a noisy image and requires determination of the clean (original) image. Inverse problems tend to generate multiple undesirable solutions because of their ill-posed nature: fewer observations than the number of system parameters under investigation. The solution of an inverse problem may be unstable, amplifying errors in the intended solution from the arbitrarily small errors in the measurement data [58].

Anisotropic diffusion has been widely used to address the ill-posed nature of inverse problems. Despite its effectiveness in image denoising, a paucity of studies exist to analyze the impact of anisotropic diffusion in other image processing techniques, such as compression, segmentation, inpainting, and tomographic image reconstruction [29]. Another possible research avenue can be the application of anisotropic diffusion in neural networks for learning a priori information [59].

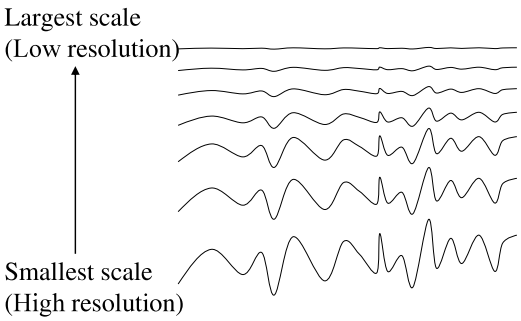

Fig. 3. One-dimensional signal at different scale resolutions.

3.5. Expansion into high-dimensional space

Most anisotropic diffusion methods focus on two-dimensional gray-scale images. In recent years, researchers have developed interest in processing higher-dimensional and vector-valued images because of the increased computational power and availability of color printers and scanners. Extending the methods into this direction will mark an important milestone in sensitive practical applications, including medical and radar imaging. This scientific inquiry requires computationally inexpensive methods for denoising higher-dimensional images without destroying semantic features.

3.6. Convergence criterion setting

The evolving solution, u, in (2.9) should be tested for optimality at every iteration. The dynamical system requires an appropriate stopping criterion to generate an optimal solution after some iterations [60–62]. The fundamental property of a criterion is that it should approach a specific preset value, upper or lower bound, as the system advances through iterations. The bound corresponds to the quality of an image. Upon meeting the criterion conditions, the generated image becomes of the highest possible quality. For image denoising problems, the optimal image at the exit point of the criterion contains minimum error corresponding to acceptable values of quality metrics (e.g., peak-signal-to-noise ratio and structural similarity).

Setting the convergence rules remains a long-standing problem in iterative methods, including those intended to remove noise in images. The primary questions are (1) at which specific point in time should we stop the iterations? (2) what is the lower/upper bound to mark the exit condition for the iterating dynamical system? how should we establish a balance between fidelity of results and computational time? These questions may stimulate scholarly discussions to address implementation challenges of iterative methods.

3.7. Relationship of features at different scale-space solutions

The denoising (diffusion) process creates a series of solutions at varied scales. Each solution corresponds to an image with features smoothed to a specific degree of resolution (Fig. 3). The solution at an infinity scale contains a constant image characterized by uniform distribution of gray levels. Image features at the lowest scale have the highest resolution, presenting well-distinguished and visually appealing structures. Fig. 2 shows a one-dimensional signal at the bottom convolved (smoothed) by a Gaussian kernel with an increasing variance from bottom to top [28,63].

Despite the well-established knowledge that diffusion leads to scale-space solutions [28], the fundamental question remains to determine the mathematical relationship of the signal features at different scales. In essence, after the convolution by a given kernel (e.g., Gaussian), how do these features relate mathematically? The relationship may

enhance our understanding on how the diffusion process works. For example, we will understand how and why pixels diffuse across image regions to reduce noise and spurious features. Furthermore, inverse operations may be established to reconstruct the original (noisy) signal after diffusion.

3.8. Implementation schemes

For decades, explicit numerical schemes have been widely applied to realize and implement partial differential equations (PDEs) for nonlinear diffusion models. These schemes provide simpler and quicker implementation strategies, but become increasingly inefficient and ineffective in time-sensitive applications that demand larger time steps. Explicit (Euler forward) schemes produce better results under the Courant–Friedrichs–Lewy (CFL) criterion [64] that restricts a time step between 0 and 0.25 to achieve stable and quality results. This restriction makes such schemes ineffective in complex computer vision and image processing tasks.

Given the limitations of explicit schemes, researchers should investigate and establish more advanced and efficient numerical methods for PDEs [29]: implicit schemes, splitting and multigrid techniques, and grid adaptation strategies. Weickert [29] argues researchers to develop advanced software packages that implement different nonlinear diffusion filters. Supporting the open science [65,66], the packages should be made publicly available across the research community.

3.9. Noise estimation

Development of regularization terms require a comprehensive knowledge of the noise statistics in an image. Effective methods for noise estimation should be devised as an important milestone to achieve robust nonlinear anisotropic diffusion models [67–70]. However, establishment of such methods seems challenging due to the random nature of noise. This open-ended research problem may be addressed using machine learning methods that can learn complex and random relationships of noise variables [71]. Also, compressive sensing and stochastic techniques [72–74] may be employed to model image noise. The fundamental question is to derive noise PDF from the corrupted image.

3.10. Image quality evaluation metrics

Quality of results generated by restoration methods, including the ones discussed in our work, should be gauged using suitable assessment metrics. Currently, most authors prefer peak-signal-to-noise ratio (PSNR) [75] and structural similarity (SSIM) [76] metrics for image quality assessment (IQA). However, PSNR and SSIM require complete information of the reference image that may not be available in practical applications [77]. When executing a real denoising problem, the original (clean) image is unavailable. In some few cases, we may have a small portion of information from the original image. Researchers may need to divert their attention to other types of metrics for image quality assessment, including reduced-reference and no-reference IQA metrics [78–83]. Subjective IQA approaches, while they remain popularly used, should not be drawn based on the author's perceptions and experience. Other people should be engaged in the quality assessment process, and voting statistics employed as the basis for drawing conclusions.

4. Proposed anisotropic diffusion method

We applied a four-point explicit numerical scheme to implement the proposed anisotropic diffusion model. The essence of this implementation is to demonstrate an important research opportunity described in Section 3.2: *design of shape-defining constant*. Specifically, the implementation highlights that setting tuning constants (of the diffusion kernel) to achieve optimal results may be a rather daunting and time-consuming process. For completeness, our model is compared with the classical Perona–Malik model.

Discretizing (2.13) under the explicit scheme yields

$$\frac{u_{ij}^{n+1}-u_{ij}^{n}}{\triangle t}=\mathrm{div}_{ij}\left(\frac{\rho'(|\nabla u_{ij}^{n}|)}{|\nabla u_{ij}^{n}|+\epsilon}\right)-\lambda\frac{u_{ij}^{n}-f_{ij}^{n}}{(u_{ij}^{n})^{2}+\epsilon} \tag{4.1}$$

where

$$\rho'(|\nabla u_{ij}^{n}|)=|\nabla u_{ij}^{n}|\begin{pmatrix}-\frac{1}{\left(\frac{|\nabla u_{ij}^{n}|}{K}+\epsilon\right)}\\ 1-a\\ -\frac{1}{\left(\frac{|\nabla u_{ij}^{n}|}{K}+\epsilon\right)}\\ 1+a\end{pmatrix} \tag{4.2}$$

and $\epsilon \ll 0^{+}$ denotes the small constant that prevents numerical instability.

Therefore,

$$u_{ij}^{n+1}=u_{ij}^{n}+\triangle t\left(\mathrm{div}_{ij}\left(\frac{\rho'(|\nabla u_{ij}^{n}|)}{|\nabla u_{ij}^{n}|+\epsilon}\right)-\lambda\frac{u_{ij}^{n}-f_{ij}^{n}}{(u_{ij}^{n}+\epsilon)^{2}}\right). \tag{4.3}$$

The parameters were set as follows: $\triangle t=0.15$ (CFL criterion), $\lambda=0.05$, $\epsilon=0.000001$. We determined the values of a and K empirically based on the quality of results. Experiments were conducted and an optimal set $\{a,K\}$ corresponding to higher values of PSNR [75] and SSIM [76] was selected. The former metric gives the signal strength relative to the noise content in the image. Higher PSNR values are preferred for quality images. Despite its wide application, PSNR lacks human perceptual qualities. SSIM, which ranges between 0 and 1, addresses this weakness by emulating the human visual system. Quality images give higher values of SSIM.

Experiments were conducted on four types of images downloaded from public domains: Pout,[1] Mandril, Walkbridge,[2] and Cat.[3] In the first experiment, speckle noise of standard deviation 25.50 was added into original images of Pout, Mandril, and Walkbridge. Next, our method was applied to remove noise from these images and the results were compared with those generated by the Perona–Malik method [28]. The second experiment focused on testing the performance of our method under heavy noise conditions. Therefore, the original image of Cat was corrupted by additive Gaussian noise of standard deviations 40, 50, and 60. Next, the methods by Monteil and Beghdadi [84], Tebini et al. [85], Gupta et al. [86], Rezgui et al. [87], and ours were applied to restore the original image. In all experiments, we applied PSNR and SSIM to gauge quality of the denoised images. Implementation codes have been shared for researchers to reproduce our results.[4]

[1] https://www.mathworks.com/help/images/image-import-and-export.html

[2] http://www.imageprocessingplace.com/root_files_V3/image_databases.htm

[3] http://www.hpca.ual.es/~vruiz/images/

[4] https://www.mathworks.com/matlabcentral/fileexchange/116260-anisotropic-diffusion-denoising

Table 2
Performance of Perona–Malik method and our method under optimal tuning parameters, $\{a, K\}$.

Method	Pout			Mandril			Walkbridge		
	PSNR	SSIM	$\{a, K\}$	PSNR	SSIM	$\{a, K\}$	PSNR	SSIM	$\{a, K\}$
Perona–Malik method [28]	33.3637	0.8738	$\{-, 5\}$	26.0017	0.8188	$\{-, 87\}$	25.2815	0.8630	$\{-, 90\}$
Our method	33.5270	0.8780	$\{7, 5\}$	26.0013	0.0.8189	$\{6, 48\}$	25.2905	0.8628	$\{9, 51\}$

Table 3
Peak-signal-to-noise ratio (PSNR) and structural similarity (SSIM) values of different anisotropic diffusion methods for the cat image corrupted by heavy Gaussian noise. (σ and t denotes standard deviation and iteration number, respectively.)

Method	$\sigma = 40, t = 30$		$\sigma = 50, t = 35$		$\sigma = 60, t = 40$	
	PSNR	SSIM	PSNR	SSIM	PSNR	SSIM
Perona–Malik method [28]	20.7438	0.4500	17.3968	0.2915	16.3042	0.2502
Monteil method [84]	22.2268	0.5824	19.8749	0.4245	18.8512	0.3624
Tebini [85]	22.9435	0.6201	20.2365	0.4582	19.0856	0.3983
Gupta method [86]	23.8332	0.6618	20.9656	0.5078	21.4205	0.5433
Rezgui et al. [87]	20.3328	0.5399	18.5991	0.4671	17.1711	0.4083
Proposed method ($a = 13, K = 19$)	$t = 5$		$t = 6$			
	23.8570	0.7668	22.5464	0.7137	21.5094	0.6683

5. Results and discussions

The current work demonstrates the capabilities of methods based on nonlinear anisotropic diffusion in restoring degraded images without destroying important features. Despite their notable advantages, potential weaknesses of these methods have been discussed to inspire early career researchers in developing more advanced and effective nonlinear anisotropic diffusion methods. We have indicated interesting research avenues in this promising field, the goal being to expand the application domain of such methods in denoising corrupted images. Supported by our experimental results, researchers may raise critical questions leading to improvement of the proposed method or other classical methods in the literature.

Results justify the capability of our approach to generate images with higher perceptual and objective qualities (Fig. 4). Compared with the results generated by the Perona–Malik method, our images contain visually appealing and attractive features. Specifically, the proposed approach suppresses noise and reconstructs visual semantic features. Even for the complex images, such as Baboon (Fig. 4, second row), our approach generates acceptable results by preserving plausible features (e.g., fur, edges, and textures). Intuitively, we can observe from the results (Fig. 4, far-right column) that the current method properly balances between visual appealingness and noise removal in accordance with the human visual system. This encouraging observation may be explained from the structure of our diffusion kernel (3.3) that it provides an effective strategy for steering the diffusion process across image regions. However, this benefit comes at the expense of tuning the kernel parameters, a and K. We noted that the image type dictates the $\{a, K\}$ search space, which seems non-intuitive as it requires heuristic approaches to determine optimal values. Future studies may consider more efficient algorithms for computing the values of a and K that produce optimal results.

The proposed method performs well on objective quality metrics (Tables 2 and 3[5]). The method gives competitive values of PSNR and SSIM even for an image with a higher noise density. More importantly, our method converges faster that other methods, thus making it more suitable in real-time computing devices. For a Cat image degraded by Gaussian noise of standard deviation 40, the proposed method converges with only five iterations—sixfold convergence rate faster than the classical methods.

Despite its higher computational speed, the tuning parameters, $\{a, K\}$, of our method needs manual tuning to achieve optimal results (Table 2). This time-consuming process may give design and implementation challenges in practical systems. The challenge may be addressed by establishing the relationship between parameters and image structural–statistical information. Machine learning and fitting techniques may be applied to establish the relationship, which should then be embedded into the diffusion kernel. As the dynamical system (4.1) advances, the parameters will be adaptively updated to steer the system towards quality results.

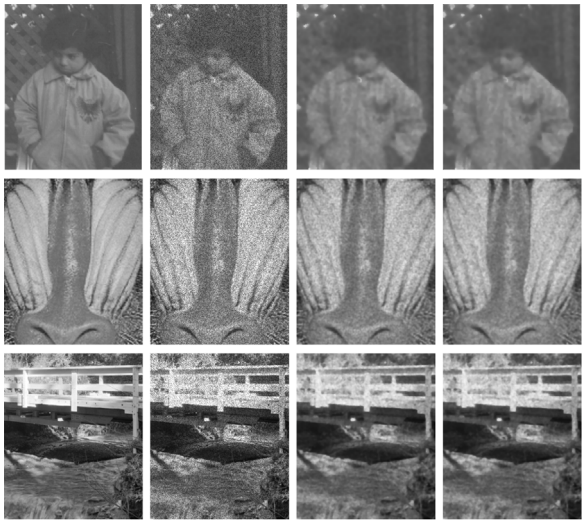

(a) Original image (b) Noisy image (c) Perona-Malik (d) Our method

Fig. 4. Noise removal from noisy images of Pout, Mandril, and Walkbridge, scaled and cropped for presentation purposes.

We observed from empirical experiments that the fractional fidelity term (2.13) by Lu et al. [39] promotes quality results for both additive and multiplicative noise. But more efforts are needed to establish superior fidelity terms that adapt to a variety of noise types, including the ones with mixed PDFs co-existing in the same image. In this regard, the proposed diffusion Eq. (2.9) may be modified as

$$\frac{\partial u}{\partial t} = \operatorname{div}\left(\frac{\rho'(|\nabla u|)}{|\nabla u|}\nabla u\right) - \sum_{i=1}^{N} \lambda_i \vartheta_i'(u, f), \tag{5.1}$$

where N denotes the number of fidelity terms dependent upon the nature and type of noise. The question remains to determine the values of λ and expressions defining $\vartheta'(u, f)$.

[5] For fair comparison, some results from this Table were adapted from the work by Gupta et al. [86].

6. Conclusion

The current work highlights potential advantages of nonlinear anisotropic diffusion methods for noise removal in corrupted images. Given their wide applications in image processing and computer vision, it seems reasonable to further improve the methods and make them more useful in theoretical and practical settings. Therefore, limitations of the methods have been extensively discussed as an attempt to create awareness and establish research opportunities within the scholarly community. Furthermore, we have proposed a nonlinear anisotropic diffusion method that generates promising results relative to the classical Perona–Malik formulation.

Declaration of competing interest

The authors declare that they have no known competing financial interests or personal relationships that could have appeared to influence the work reported in this paper.

Data availability

The link to the implementation source code has been included in the manuscript. https://www.mathworks.com/matlabcentral/fileexchange/116260-anisotropic-diffusion-denoising

Acknowledgment

This work is not funded by any organization.

References

[1] Shen H, Li X, Zhang L, Tao D, Zeng C. Compressed sensing-based inpainting of aqua moderate resolution imaging spectroradiometer band 6 using adaptive spectrum-weighted sparse bayesian dictionary learning. IEEE Trans Geosci Remote Sens 2013;52:894–906.
[2] Karaoğu O, Bilge HŞ, Uluer İ. Removal of speckle noises from ultrasound images using five different deep learning networks. Eng Sci Technol 2022;29:101030.
[3] Pang T, Zheng H, Quan Y, Ji H. Recorrupted-to-recorrupted: Unsupervised deep learning for image denoising. In: Proceedings of the IEEE/CVF conference on computer vision and pattern recognition. 2021, p. 2043–52.
[4] Buades A, Coll B, Morel J-M. A review of image denoising algorithms, with a new one. Multiscale Model Simul 2005;4:490–530.
[5] Buades A, Coll B, Morel J-M. Image denoising methods. A new nonlocal principle. SIAM Rev 2010;52:113–47.
[6] Jain P, Tyagi V. A survey of edge-preserving image denoising methods. Inf Syst Front 2016;18:159–70.
[7] Tian C, Fei L, Zheng W, Xu Y, Zuo W, Lin C-W. Deep learning on image denoising: An overview. Neural Netw 2020;131:251–75.
[8] Gondara L. Medical image denoising using convolutional denoising autoencoders. In: 2016 IEEE 16th international conference on data mining workshops. IEEE; 2016, p. 241–6.
[9] Starck J-L, Candès EJ, Donoho DL. The curvelet transform for image denoising. IEEE Trans Image Process 2002;11:670–84.
[10] Ilesanmi AE, Ilesanmi TO. Methods for image denoising using convolutional neural network: A review. Complex Intell Syst 2021;7:2179–98.
[11] Shi Q, Tang X, Yang T, Liu R, Zhang L. Hyperspectral image denoising using a 3-D attention denoising network. IEEE Trans Geosci Remote Sens 2021;59:10348–63.
[12] Zhang J, Cao L, Wang T, Fu W, Shen W. NHNet: A non-local hierarchical network for image denoising. IET Image Process 2022a;16:2446–56.
[13] Zhang J, Cai Z, Chen F, Zeng D. Hyperspectral image denoising via adversarial learning. Remote Sens 2022b;14:1790.
[14] Fu B, Zhao X, Song C, Li X, Wang X. A salt and pepper noise image denoising method based on the generative classification. Multimedia Tools Appl 2019;78:12043–53.
[15] Russo F. A method for estimation and filtering of gaussian noise in images. IEEE Trans Instrum Meas 2003;52:1148–54.
[16] Luisier F, Blu T, Unser M. Image denoising in mixed Poisson–Gaussian noise. IEEE Trans Image Process 2010;20:696–708.
[17] Zhang B, Fadili JM, Starck J-L. Wavelets, ridgelets, and curvelets for Poisson noise removal. IEEE Trans Image Process 2008;17:1093–108.
[18] Jin Q, Grama I, Liu Q. Poisson shot noise removal by an oracular non-local algorithm. J Math Imaging Vision 2021;63:855–74.
[19] Yu J, Chen L, Zhou S, Wang L, Li H, Huang S. Adaptive image denoising for speckle noise images based on fuzzy logic. Int J Imaging Syst Technol 2020;30:1132–42.
[20] Fan L, Zhang F, Fan H, Zhang C. Brief review of image denoising techniques. Vis Comput Ind Biomed Art 2019;2:1–12.
[21] Thanh D, Surya P, et al. A review on CT and X-ray images denoising methods. Informatica 2019;43.
[22] Hajiaboli MR. An anisotropic fourth-order diffusion filter for image noise removal. Int J Comput Vis 2011;92:177–91.
[23] Buades A, Coll B, Morel JM. On image denoising methods. CMLA Prepr 2004;5:19–26.
[24] Mamaev N, Yurin D, Krylov A. Finding the parameters of a nonlinear diffusion denoising method by ridge analysis. Comput Math Model 2018;29:334–43.
[25] Deng L, Zhu H, Yang Z, Li Y. Hessian matrix-based fourth-order anisotropic diffusion filter for image denoising. Opt Laser Technol 2019;110:184–90.
[26] Kumar S, Alam K, Chauhan A. Fractional derivative based nonlinear diffusion model for image denoising. SeMA J 2021;1–10.
[27] Chen Y, Vemuri BC, Wang L. Image denoising and segmentation via nonlinear diffusion. Comput Math Appl 2000;39:131–49.
[28] Perona P, Malik J. Scale-space and edge detection using anisotropic diffusion. IEEE Trans Pattern Anal Mach Intell 1990;12:629–39.
[29] Weickert J. Anisotropic diffusion in image processing, vol. 1. Teubner Stuttgart; 1998.
[30] Tikhonov A. Solutions of ill-posed problems, vol. 151. Wiley; 1977.
[31] Rudin LI, Osher S, Fatemi E. Nonlinear total variation based noise removal algorithms. Physica D 1992;60:259–68.
[32] Charbonnier P, Blanc-Feraud L, Aubert G, Barlaud M. Two deterministic half-quadratic regularization algorithms for computed imaging. In: Proceedings of 1st international conference on image processing, vol. 2, IEEE; 1994, p. 168–72.
[33] Rey WJ. Introduction to robust and quasi-robust statistical methods. Springer Science & Business Media; 2012.
[34] Huber PJ. Robust statistics. In: International encyclopedia of statistical science. Springer; 2011, p. 1248–51.
[35] Ganan S, McClure D. Bayesian image analysis: An application to single photon emission tomography. Amer Statist Assoc 1985;12–8.
[36] Geman S. Statistical methods for tomographic image reconstruction. Bull Int Stat Inst 1987;4:5–21.
[37] Dennis Jr JE, Welsch RE. Techniques for nonlinear least squares and robust regression. Comm Statist Simulation Comput 1978;7:345–59.
[38] Beaton AE, Tukey JW. The fitting of power series, meaning polynomials, illustrated on band-spectroscopic data. Technometrics 1974;16:147–85.
[39] Lu J, Shen L, Xu C, Xu Y. Multiplicative noise removal in imaging: An exp-model and its fixed-point proximity algorithm. Appl Comput Harmon Anal 2016;41:518–39.
[40] Guo Z, Sun J, Zhang D, Wu B. Adaptive Perona–Malik model based on the variable exponent for image denoising. IEEE Trans Image Process 2011;21:958–67.
[41] Wielgus M. Perona-malik equation and its numerical properties. 2014, arXiv preprint arXiv:1412.6291.
[42] Tsiotsios C, Petrou M. On the choice of the parameters for anisotropic diffusion in image processing. Pattern Recognit 2013;46:1369–81.
[43] Maiseli B, Msuya H, Kessy S, Kisangiri M. Perona–Malik model with self-adjusting shape-defining constant. Inform Process Lett 2018;137:26–32.
[44] You Y-L, Xu W, Tannenbaum A, Kaveh M. Behavioral analysis of anisotropic diffusion in image processing. IEEE Trans Image Process 1996;5:1539–53.
[45] Gao M, Kang B, Feng X, Zhang W, Zhang W. Anisotropic diffusion based multiplicative speckle noise removal. Sensors 2019;19:3164.
[46] Jidesh P, Bini A. A complex diffusion driven approach for removing data-dependent multiplicative noise. In: International conference on pattern recognition and machine intelligence. Springer; 2013, p. 284–9.
[47] Hao Y, Xu J, Li S, Zhang X. A variational model based on split bregman method for multiplicative noise removal. AEU-Int J Electron Commun 2015;69:1291–6.
[48] Zhang Y, Li S, Guo Z, Wu B, Du S. Image multiplicative denoising using adaptive euler's elastica as the regularization. J Sci Comput 2022;90:1–34.
[49] Kumar S, Kumar N, Alam K. A nonlinear anisotropic diffusion equation for image restoration with forward–backward diffusivities. Recent Adv Electr Electron Eng 2021;14:428–34.
[50] Jain SK, Ray RK. Non-linear diffusion models for despeckling of images: Achievements and future challenges. IETE Tech Rev 2020;37:66–82.
[51] Boyat AK, Joshi BK. A review paper: Noise models in digital image processing. 2015, arXiv preprint arXiv:1505.03489.
[52] Boncelet C. Image noise models. In: The essential guide to image processing. Elsevier; 2009, p. 143–67.
[53] Scherzer O, Grasmair M, Grossauer H, Haltmeier M, Lenzen F. Image and noise models. In: Variational methods in imaging. Springer; 2009, p. 27–49.
[54] Gilboa G, Sochen N, Zeevi YY. Texture preserving variational denoising using an adaptive fidelity term. In: Proc. VLsM, vol. 3, 2003.
[55] Vogel CR. Computational methods for inverse problems. SIAM; 2002.
[56] Engl HW, Hanke M, Neubauer A. Regularization of inverse problems, vol. 375. Springer Science & Business Media; 1996.

[57] Romanov VG. Inverse problems of mathematical physics. In: Inverse problems of mathematical physics. De Gruyter; 2018.
[58] Kabanikhin SI. Definitions and examples of inverse and ill-posed problems. 2008.
[59] Singh P, Shankar A. A novel optical image denoising technique using convolutional neural network and anisotropic diffusion for real-time surveillance applications. J Real-Time Image Process 2021;18:1711–28.
[60] Landi G, Piccolomini EL, Tomba I. A stopping criterion for iterative regularization methods. Appl Numer Math 2016;106:53–68.
[61] Rao K, Malan P, Perot JB. A stopping criterion for the iterative solution of partial differential equations. J Comput Phys 2018;352:265–84.
[62] Axelsson O, Kaporin I. Error norm estimation and stopping criteria in preconditioned conjugate gradient iterations. Numer Linear Algebra Appl 2001;8:265–86.
[63] Witkin AP. Scale-space filtering. In: Readings in computer vision. Elsevier; 1987, p. 329–32.
[64] Courant R, Friedrichs K, Lewy H. On the partial difference equations of mathematical physics. IBM J Res Dev 1967;11:215–34.
[65] Vicente-Saez R, Martinez-Fuentes C. Open science now: A systematic literature review for an integrated definition. J Bus Res 2018;88:428–36.
[66] Foster ED, Deardorff A. Open science framework (OSF). J Med Libr Assoc 2017;105:203.
[67] Pimpalkhute VA, Page R, Kothari A, Bhurchandi KM, Kamble VM. Digital image noise estimation using DWT coefficients. IEEE Trans Image Process 2021;30:1962–72.
[68] Sarker R, Kaur A, Singh D. Noise estimation using back propagation neural networks. ECS Trans 2022;107:18761.
[69] San-Roman R, Nachmani E, Wolf L. Noise estimation for generative diffusion models. 2021, arXiv preprint arXiv:2104.02600.
[70] Pyatykh S, Hesser J, Zheng L. Image noise level estimation by principal component analysis. IEEE Trans Image Process 2012;22:687–99.
[71] Zhang X-P. Thresholding neural network for adaptive noise reduction. IEEE Trans Neural Netw 2001;12:567–84.
[72] Leportier T, Park M-C. Filter for speckle noise reduction based on compressive sensing. Opt Eng 2016;55:121724.
[73] Bindilatti AA, Mascarenhas ND. A nonlocal Poisson denoising algorithm based on stochastic distances. IEEE Signal Process Lett 2013;20:1010–3.
[74] Isogawa K, Ida T, Shiodera T, Takeguchi T. Deep shrinkage convolutional neural network for adaptive noise reduction. IEEE Signal Process Lett 2017;25:224–8.
[75] Wang Z, Bovik AC. Mean squared error: Love it or leave it? A new look at signal fidelity measures. IEEE Signal Process Mag 2009;26:98–117.
[76] Wang Z, Bovik AC, Sheikh HR, Simoncelli EP. Image quality assessment: From error visibility to structural similarity. IEEE Trans Image Process 2004;13:600–12.
[77] Ding K, Ma K, Wang S, Simoncelli EP. Comparison of full-reference image quality models for optimization of image processing systems. Int J Comput Vis 2021;129:1258–81.
[78] Wu J, Lin W, Shi G, Liu A. Reduced-reference image quality assessment with visual information fidelity. IEEE Trans Multimed 2013;15:1700–5.
[79] Wang Z, Simoncelli EP. Reduced-reference image quality assessment using a wavelet-domain natural image statistic model. In: Human vision and electronic imaging X, vol. 5666, SPIE; 2005, p. 149–59.
[80] Rehman A, Wang Z. Reduced-reference image quality assessment by structural similarity estimation. IEEE Trans Image Process 2012;21:3378–89.
[81] Bosse S, Maniry D, Müller K-R, Wiegand T, Samek W. Deep neural networks for no-reference and full-reference image quality assessment. IEEE Trans Image Process 2017;27:206–19.
[82] Kang L, Ye P, Li Y, Doermann D. Convolutional neural networks for no-reference image quality assessment. In: Proceedings of the IEEE conference on computer vision and pattern recognition. 2014, p. 1733–40.
[83] Mittal A, Moorthy AK, Bovik AC. No-reference image quality assessment in the spatial domain. IEEE Trans Image Process 2012;21:4695–708.
[84] Monteil J, Beghdadi A. A new interpretation and improvement of the nonlinear anisotropic diffusion for image enhancement. IEEE Trans Pattern Anal Mach Intell 1999;21:940–6.
[85] Tebini S, Seddik H, Braiek EB. An advanced and adaptive mathematical function for an efficient anisotropic image filtering. Comput Math Appl 2016;72:1369–85.
[86] Gupta B, Lamba SS, et al. An efficient anisotropic diffusion model for image denoising with edge preservation. Comput Math Appl 2021;93:106–19.
[87] Rezgui H, Maouni M, Hadji ML, Touil G. Three robust edges stopping functions for image denoising. Bol Soc Paran Mat 2022;40:1–12.